



# Accelerating NLTE radiative transfer by means of the Forth-and-Back Implicit Lambda Iteration: A two-level atom line formation in 2D Cartesian coordinates

Ivan Milić<sup>a,b,\*</sup>, Olga Atanacković<sup>c</sup>

<sup>a</sup> *Astronomical Observatory, Volgina 7, 11060 Belgrade, Serbia*

<sup>b</sup> *J. L. Lagrange Laboratory, UMR 7293, Université de Nice Sophia Antipolis, CNRS, Observatoire de la Côte d'Azur, Campus Valrose, 06108 Nice, France*

<sup>c</sup> *Department of Astronomy, Faculty of Mathematics, University of Belgrade, Studentski trg 16, 11000 Belgrade, Serbia*

Received 5 July 2013; received in revised form 7 April 2014; accepted 24 May 2014

Available online 4 June 2014

## Abstract

State-of-the-art methods in multidimensional NLTE radiative transfer are based on the use of local approximate lambda operator within either Jacobi or Gauss–Seidel iterative schemes. Here we propose another approach to the solution of 2D NLTE RT problems, Forth-and-Back Implicit Lambda Iteration (FBILI), developed earlier for 1D geometry. In order to present the method and examine its convergence properties we use the well-known instance of the two-level atom line formation with complete frequency redistribution. In the formal solution of the RT equation we employ short characteristics with two-point algorithm. Using an implicit representation of the source function in the computation of the specific intensities, we compute and store the coefficients of the linear relations  $J = a + bS$  between the mean intensity  $J$  and the corresponding source function  $S$ . The use of iteration factors in the ‘local’ coefficients of these implicit relations in two ‘inward’ sweeps of 2D grid, along with the update of the source function in other two ‘outward’ sweeps leads to four times faster solution than the Jacobi’s one. Moreover, the update made in all four consecutive sweeps of the grid leads to an acceleration by a factor of 6–7 compared to the Jacobi iterative scheme.

© 2014 COSPAR. Published by Elsevier Ltd. All rights reserved.

**Keywords:** Radiative transfer; Line formation; Numerical techniques

## 1. Introduction

Radiative transfer (RT) is at the heart of many astrophysical problems. In order to interpret the observed spectra of astrophysical objects it is essential to solve the RT problem. Radiation not only carries the information on the physical state of the medium but also determines its structure and properties. Above all, it plays a fundamental role in the energy and force balance within the medium.

Hence the need to take it into account in modern 3D (magneto) hydrodynamic simulations (see, e.g. Hayek et al., 2010). NLTE RT problems are very demanding because of their non-local nature: radiation is decoupled from the local thermal state of the gas via scattering processes, so that the state of the gas at one point in the medium depends, via radiative processes, on the state of the gas at all other points. In order to compute emergent intensity in spectral lines (or, in general, the whole set of Stokes coefficients) from a given atmospheric model (with a given run of temperature and pressure/density), the coupled equations of radiative transfer and statistical equilibrium have to be solved. The coupling of the atomic level populations and the radiation fields in the corresponding spectral line

\* Corresponding author at: Astronomical Observatory, Volgina 7, 11060 Belgrade, Serbia. Tel.: +381 63272988.

E-mail addresses: [milic@aob.rs](mailto:milic@aob.rs) (I. Milić), [olga@matf.bg.ac.rs](mailto:olga@matf.bg.ac.rs) (O. Atanacković).

transitions is generally highly non-linear. Because of all that, the specific intensity of radiation, which fully describes the radiation field, is a function of seven variables: three spatial and two angular coordinates, frequency and time. Even if we neglect the time dependence in the line transfer problems, and if we discretize all the variables using a grid of 100 points for each of them, we have the specific intensity characterized by  $10^{12}$  values. Thus, the solution of the RT problem is very time and memory consuming.

Due to these difficulties, NLTE RT problems have usually been restricted to 1D geometry. However, for many objects (e.g. inhomogeneous stellar atmospheres, rotating stars, accretion disks, solar prominences) the plane-parallel or spherically symmetric 1D approximation is inadequate. Although the theoretical formulation of the multidimensional problem does not differ too much from 1D case, the computational cost is increased by many orders of magnitude. The direct solutions involving the inversion of huge matrices are rather costly, while the most simple iterative procedure, so-called  $\Lambda$  iteration,<sup>1</sup> that solves the problem equations in turn, is usually too slow to be of practical use (for discussion on its convergence properties see, e.g. Mihalas, 1978). Thus only fast iterative algorithms enable efficient solution of multidimensional NLTE RT problems with the short characteristics (SC) method almost exclusively used for the formal solution. Mihalas et al. (1978) were the first to apply the SC technique for the solution of RT in 2D slab geometries by using the difference approximation of the second-order differential equations. Kunasz and Auer (1988) developed an algorithm for the formal solution based on the SC solution of the first order differential RT equations and parabolic approximation of the source function. This SC technique was widely exploited in the last three decades within so-called ALI (Accelerated Lambda Iteration) methods, based on the operator perturbation technique (for a review see Hubeny, 2003). Probably the most commonly used ALI method is the Jacobi iteration scheme that employs the diagonal (local) part of the exact  $\Lambda$  operator as an approximate lambda operator (ALO) and computes the error introduced by this approximation iteratively (Olson et al., 1986). It has been extended to NLTE line transfer in 2D (see e.g. Kunasz and Olson, 1988; Auer and Paletou, 1994; van Noort et al., 2002), and to polarized line RT: in 1D (Faurobert-Scholl et al., 1997), in 2D cylindrical geometry (Milić, 2013), and in 3D with partial frequency redistribution (PRD) taken into account (Anusha and Nagendra, 2011). The convergence rate of the Jacobi method was usually increased by the Ng acceleration technique (Ng, 1974). The Gauss-Seidel method is twice as fast as the Jacobi method, being usually further accelerated by the successive overrelaxation (SOR) technique (Trujillo Bueno and Fabiani Bendicho, 1995). It

was generalized to the 2D line transfer problem by Léger et al. (2007). Another very fast approach is the bi-conjugate gradient method (e.g. Papkalla, 1995) that has been recently generalized to the multidimensional polarized line transfer with PRD by Anusha et al. (2011).

Here we propose another approach to the solution of 2D NLTE radiative transfer problems. Our aim is to generalize to 2D geometry the Forth-and-Back Implicit Lambda Iteration – FBILI, previously developed for NLTE line transfer problems in 1D in the paper by Atanacković-Vukmanović et al. (1997), hereinafter ACS97. For simplicity, in this paper we shall use two-level atom model. The multilevel atom case in 1D is considered by ACS97 and the transition from 1D to 2D will be described in a forthcoming paper. The FBILI is an extremely fast method that, without additional acceleration technique, significantly outperforms available methods in 1D problems (for its convergent properties and the problems solved, see Atanacković-Vukmanović, 2007). A very fast convergence to the exact solution is achieved by the iterative computation of the coefficients of implicit linear relations between the in-going radiation field intensities and the line source function during the forward sweep of the 1D grid and by their use in updating the source function together with the out-going specific intensities during the backward sweep. Moreover, the use of an iteration factor in the ‘local’ coefficient of the implicit linear relations enormously increases the convergence rate (for details see Section 2).

We recall the basic idea of the FBILI method in the solution of NLTE line formation in 1D geometry in Section 2. The implementation of the FBILI method to 2D Cartesian geometry is described in Section 3. In Section 4 we solve a simple test problem and discuss the results, and in Section 5 we comment on our future work.

## 2. Forth-and-Back Implicit Lambda Iteration (FBILI) basics

The FBILI method is developed and fully described in the paper by ACS97. The essential features of this approach are the following:

- Two-point boundary nature of the problem, i.e. the existence of two separate families of boundary conditions naturally suggests the separate description of the propagation of the in-going intensities of the radiation field  $I_{\nu\mu}^-$  with initial conditions at the surface and that of the out-going intensities  $I_{\nu\mu}^+$  with initial conditions at the bottom of the system. This recalls the basic idea of a forth-and-back scheme.
- The physics of radiative transfer is almost linear, hence a linear algorithm is feasible for the solution of the problem.
- An implicit representation of the source function is used in the computation of both the in-going and the out-going intensities with a piecewise parabolic behavior of the source function as a suitable assumption.

<sup>1</sup>  $\Lambda$  operator was firstly introduced by Schwarzschild as the operator acting on the source function to give the mean intensity.

Before we present the FBILI algorithm in more detail let us stress here the main reason for its high convergence. As well-known the slow convergence of the classical Lambda iteration is due to the fact that it computes the *total* mean intensity  $J(\tau)$  from the old source function  $S^o(\tau)$ , keeping thus from the previous iteration more information than necessary. Apart from using the two-stream representation of the radiation field, the FBILI method splits the mean intensities  $J^-(\tau)$  and  $J^+(\tau)$  into the local and non-local components, with the local parts linearly dependent on the unknown local values of the source function  $S(\tau)$  and its derivative  $S'(\tau)$ . At each iterative step only the non-local part of the in-going mean intensity  $J^-(\tau)$  is computed from the old values  $S^o(\tau)$  in the forward sweep of 1D grid, whereas the non-local part of  $J^+(\tau)$  and the local part of both  $J^-(\tau)$  and  $J^+(\tau)$  are computed from the updated values of  $S(\tau)$  in the backward sweep. The fact that the only peace of information transferred from the previous iteration is contained in the non-local part of the in-going mean intensity  $J^-(\tau)$  ensures an extremely high convergence rate of the FBILI method.

In order to demonstrate the FBILI approach, we shall consider the two-level atom line transfer with complete frequency redistribution in a static and isothermal plane-parallel 1D medium with no background continuum. Under these assumptions, the RT equation takes the form:

$$\mu \frac{dI_{\nu\mu}(\tau)}{d\tau} = \phi_\nu [I_{\nu\mu}(\tau) - S(\tau)], \quad (1)$$

where  $I_{\nu,\mu}(\tau)$  is the specific intensity of the radiation field at the mean optical depth  $\tau$ , at frequency  $\nu$  and direction  $\mu$  ( $\mu$  is the cosine of the angle between the photon's direction and the outward normal). The absorption-line profile,  $\phi_\nu$ , is normalized to unity. The frequency independent line source function is

$$S(\tau) = \varepsilon B + (1 - \varepsilon)J(\tau), \quad (2)$$

where  $\varepsilon$  is the photon destruction probability,  $B$  is the Planck function, and

$$J(\tau) = \frac{1}{2} \int_{-\infty}^{\infty} \phi_\nu d\nu \int_{-1}^1 I_{\nu\mu}(\tau) d\mu \quad (3)$$

is the scattering integral.

The specific intensities incident onto the boundaries, i.e. the in-going intensities  $I_{\nu\mu}^-(\tau = 0)$  incident onto the surface and the out-going intensities  $I_{\nu\mu}^+(\tau = T)$  incident onto the bottom of the medium, are considered as given.

In the numerical solution of the RT equation (1), the discrete set of specific intensities with frequencies  $\nu_i$ ,  $i = 1, NF$ , and directions  $\mu_j$ ,  $j = 1, ND$  is considered, and all the relevant depth-dependent functions are evaluated on a finite grid of the mean optical depth values  $\tau_l$ ,  $l = 1, NL$ .

The propagation of the unknown radiation field “along a ray” can be represented by using the integral form of the RT equation

$$I_{\nu\mu}(\tau_l) = I_{\nu\mu}(\tau_{l-1})e^{-\Delta} + \int_0^\Delta S(t)e^{t-\Delta} dt, \quad (4)$$

and by adopting a polynomial representation for the source function  $S(\tau)$  between two successive depth points  $l-1$  and  $l$ . Here,  $\Delta = \Delta\tau\phi_\nu/\mu$  is the monochromatic optical path between the two points, with  $\Delta\tau = \tau_l - \tau_{l-1}$ .

Assuming a piecewise parabolic behavior for the source function we can rewrite the RT equation (4) for the in-going intensities in the following form:

$$I_l^- = I_{l-1}^- e^{-\Delta} + q_l^- S_{l-1} + p_l^- S_l + r_l^- S_l'. \quad (5)$$

Thus we get an implicit linear relation between the in-going specific intensities and yet unknown local source function  $S_l$  and its derivative  $S_l'$ . For brevity, in Eq. (5) we omitted the dependence of  $I$  on  $\nu$  and  $\mu$ , and we put the depth index as the subscript of all depth-dependent quantities. The coefficients  $p_l^-$ ,  $q_l^-$  and  $r_l^-$  are given in the Appendix of ACS97 (the reader should note that the notation here is different from that used in the paper), and by Eq. (20) of this paper as well. They depend only on the optical distance  $\Delta$ . The first two terms on the right-hand side of Eq. (5) represent the non-local part of the in-going specific intensity, which is the only one that depends linearly on the old values of the source function at all optical depths  $\tau < \tau_l$ . Proceeding from the given boundary condition for the in-going intensities at the surface ( $I_1^-$  is usually assumed to be zero), the explicit values of all other intensities  $I_{l-1}^-$  are obtained by previous recursive application of Eq. (5) with the old values of  $S(\tau)$  and  $S'(\tau)$  at  $\tau < \tau_l$ . The derivatives  $S'(\tau)$  at  $\tau_l$  ( $l = 2, NL - 1$ ) are computed by using Lagrangian interpolation of the second order at three successive points, whereas the linear behavior of  $S(\tau)$  is assumed in the boundary layers.

By grouping together the known terms and integrating Eq. (5) over frequencies and directions, we obtain a local implicit linear relation:

$$J_l^- = a_l^- + b_l^- S_l + c_l^- S_l'. \quad (6)$$

We compute the coefficients  $a_l^-$ ,  $b_l^-$  and  $c_l^-$ , and store them for further use in the backward process of computation of the new values of  $S(\tau)$ .

In the backward process, using the integral form of the RT equation for the out-going intensities we can write

$$\begin{aligned} I_l^+ &= I_{l+1}^+ e^{-\Delta} + \int_0^\Delta S(t)e^{t-\Delta} dt \\ &= I_{l+1}^+ e^{-\Delta} + q_l^+ S_{l+1} + p_l^+ S_l + r_l^+ S_{l+1}'. \end{aligned} \quad (7)$$

Here again we assume piecewise parabolic behavior of the source function within each layer ( $\tau_l, \tau_{l+1}$ ). The coefficients  $p_l^+$ ,  $q_l^+$  and  $r_l^+$  are given in the Appendix of ACS97.

We start from the bottom layer where the out-going specific intensities  $I_{NL}^+$  are given, and consequently  $J_{NL}^+$  is known.

By taking into account Eq. (6) for  $J_{NL}^-$ , we derive a similar relation for  $J_{NL}$ . Therefrom, after having eliminated the derivative  $S_{NL}'$  according to

$$S'_{NL-1} = S'_{NL} = [S_{NL} - S_{NL-1}]/\Delta\tau, \tag{8}$$

we obtain the coefficients  $a_{NL}$ ,  $b_{NL}$  and  $c_{NL}$  of the linear relationship

$$J_{NL} = a_{NL} + b_{NL}S_{NL} + c_{NL}S_{NL-1}. \tag{9}$$

On the other hand, Eq. (6) and angle and line frequency integrated Eq. (7), the both applied to the point  $l = NL - 1$ , together with Eq. (8) allow us to express  $J_{NL-1}$  also as a linear combination of  $S_{NL}$  and  $S_{NL-1}$  with the known coefficients:

$$J_{NL-1} = a_{NL-1} + b_{NL-1}S_{NL} + c_{NL-1}S_{NL-1}. \tag{10}$$

Substituting Eqs. 9 and 10 into Eq. (2) for  $\tau_{NL}$  and  $\tau_{NL-1}$ , respectively, we can easily derive the new values of  $S_{NL}$  and  $S_{NL-1}$ . The source function derivatives  $S'_{NL}$  and  $S'_{NL-1}$  are obtained from Eq. (8), and the out-going intensities  $I_{NL-1}^+$  from Eq. (7).

Let us note that when solving the RT problem in a constant property, semi-infinite medium (the usual test problem), we take that  $J_{NL}^+ = S_{NL}$  and  $S'_{NL} = 0$ , hence immediately updating the source function according to:

$$S_{NL} = \frac{\varepsilon B + (1 - \varepsilon)a_{NL}^-}{1 - (1 - \varepsilon)(b_{NL}^- + 1)}. \tag{11}$$

For each successive upper depth point we proceed as follows. The coefficients of the relation for  $J_l^-$  (Eq. (6)) are known from the forward process. Since we assume parabolic behavior of the source function, we can use the relation

$$S'_l = \frac{2}{\Delta\tau} [S_{l+1} - S_l] - S'_{l+1}, \tag{12}$$

to express  $S'_l$  in terms of the known (just updated) values of  $S_{l+1}$  and  $S'_{l+1}$  and the thus far unknown  $S_l$ . Using Eq. (12) we can eliminate the derivative  $S'_l$  from Eq. (6) to get  $J_l^-$  as a linear function of  $S_l$  only. Integrating the formal solution for  $I_l^+$  (Eq. (7)) and taking into account that all the terms except  $S_l$  are known, similar expression for  $J_l^+$  is straightforwardly derived. Consequently, for each depth point  $\tau_l$  we obtain the linear relation

$$J(\tau) = a + bS(\tau) \tag{13}$$

that together with Eq. (2) allows us to derive the new value of  $S_l$ . With new source function  $S_l$  we can compute new derivative  $S'_l$  using Eq. (12) and  $I_l^+$  using Eq. (7). So the computation of the new source function together with the outgoing intensities is performed during the backward process layer by layer to the surface.

Let us stress here that the iterative computation of the coefficients of the implicit relations, rather than that of the intensities themselves, provides a high convergence rate. A much higher convergence rate is achieved by the use of the iteration factor  $(I_{l-1}^- e^{-\Delta} + q_l^- S_{l-1})/S_l^o$  in the 'local' coefficient (coefficient of the local source function  $S_l$ ) of Eq. (5):

$$I_l^- = \left( \frac{I_{l-1}^- e^{-\Delta} + q_l^- S_{l-1}}{S_l^o} + p_l^- \right) S_l + r_l^- S'_l. \tag{14}$$

In other words, during the forward process at each depth  $\tau_l$  we retain, for further use in the back-substitution, the ratio of the non-local part of the in-going intensity to the value of the current local source function  $S_l^o$ . It represents the only piece of information transferred from the previous iteration. This ratio of two homologous quantities is a good quasi-invariant iteration factor, which plays a very important role in accelerating the iterative procedure. It quickly attains its exact value and leads to the exact solution of the whole procedure with an extremely high convergence rate.

### 3. FBILI method in 2D

In this Section we shall describe how FBILI method can be implemented in the case of 2D medium in Cartesian geometry.

For simplicity we shall consider again two-level atom line transfer with complete frequency redistribution in a static isothermal medium with no background continuum. Let us assume that the medium is infinite and homogeneous in the  $z$ -direction, so that we solve the RT equation in the  $(x, y)$  plane (see Fig. 1) in the 'along the ray' form:

$$\frac{dI(x, y, \theta, \varphi, \nu)}{d\tau_s} = \phi(\nu)[I(x, y, \theta, \varphi, \nu) - S(x, y)]. \tag{15}$$

In order to discretize the RT equation we choose a 2D irregularly spaced spatial grid with  $NX$  points in the  $x$ -direction and  $NY$  points in the  $y$ -direction. The direction of propagation of the photons is given by the polar angle  $\theta$ , measured with respect to the  $z$ -axis, and the azimuthal

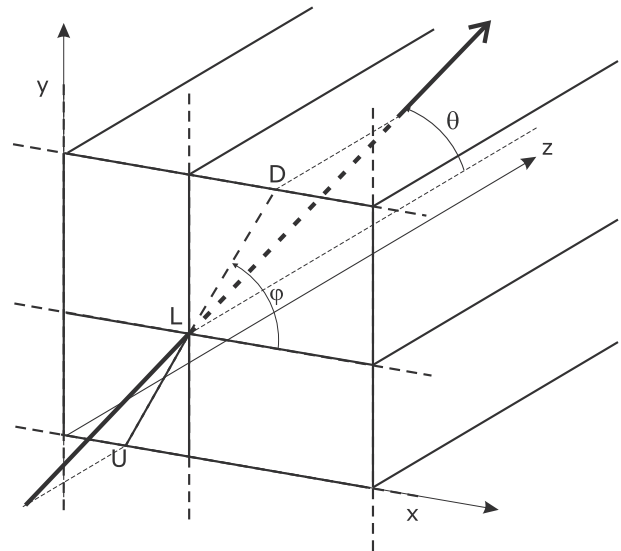


Fig. 1. Ray propagation and the definition of angles in 2D geometry. The short characteristics at grid point  $L$  for a ray propagating from the lower left intersects the cell boundaries at upwind point  $U$  and downwind point  $D$ .

angle  $\varphi$ , measured with respect to the  $x$ -axis. The normalized line absorption profile  $\phi(v)$  for pure Doppler-broadening is given by the Gaussian profile function  $\phi(v) = \frac{1}{\sqrt{\pi}\Delta v_D} e^{-(v-v_0)^2/\Delta v_D^2}$ , and  $d\tau_s$  is the line integrated optical path length along the ray.

The two-level atom line source function in 2D is given by:

$$S(x, y) = \varepsilon B + (1 - \varepsilon) J(x, y) \\ = \varepsilon B + (1 - \varepsilon) \frac{1}{4\pi} \\ \times \int_{-\infty}^{\infty} \phi(v) dv \oint I(x, y, \theta, \varphi, v) d\Omega, \quad (16)$$

where  $d\Omega = \sin \theta d\theta d\varphi$ .

Here we will describe how we can solve the problem equations (15) and (16) using the basic ideas of FBILI. Since the formal solution of the RT equation is at the heart of each iterative method we will first present it as given by ACS97.

### 3.1. Formal solution

In 2D geometry the formal solution of the RT equation is obtained by sweeping the grid four times. We label with  $k = 1, 2, 3, 4$  the four sweeps in the corresponding quadrants of the  $x - y$  coordinate system (see Fig. 2). Let us denote by  $k = 1$  the sweep that includes the directions of the specific intensity corresponding to  $0 < \varphi < \pi/2$  (i.e. the sweep characterized by increasing  $x$  and  $y$ ); by  $k = 2$  the sweep that includes the directions corresponding to  $\pi/2 < \varphi < \pi$  (i.e. the sweep characterized by decreasing  $x$  and increasing  $y$ ), etc. We take that  $y = 0$  is the surface of the medium closer to the observer. We will refer to the directions corresponding to the sweeps 1 and 2 as “inward” and those corresponding to the sweeps 3 and 4 as “outward.”

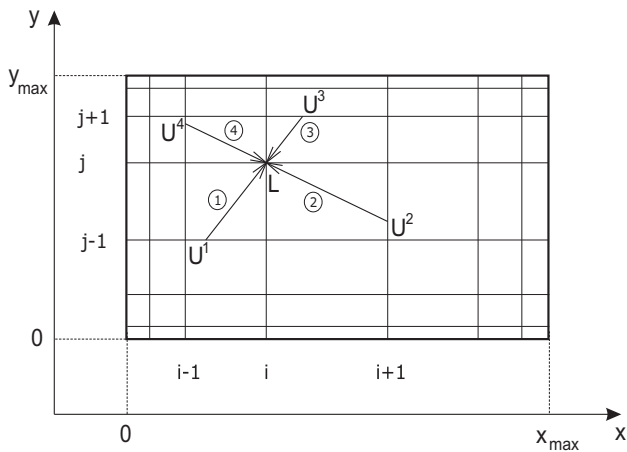


Fig. 2. Four sweeps through the local point  $L$  of 2D grid in  $(x, y)$  plane. Short characteristics and the corresponding upwind points  $U^1 - U^4$  are indicated.

Like in most of the contemporary methods, we combine the integral form of the radiative transfer equation for its formal solution with the so-called short characteristics approach. In 2D geometry, for each sweep we can rewrite Eq. (4) in the following form:

$$I_L = I_U e^{-\Delta} + \int_0^{\Delta} S(t) e^{t-\Delta} dt. \quad (17)$$

For simplicity’s sake we dropped the sweep index  $k$ . Here  $\Delta$  denotes the monochromatic optical path between the local grid point  $L = (i, j)$ , i.e. the point where the specific intensity is to be computed, and the “upwind” point  $U$ , namely the point of intersection between the direction of propagation of the ray and the nearest previous grid line (see Figs. 1 and 2). The integral in Eq. (17) can be solved analytically if we assume some polynomial representation of the source function on each given subinterval. In the standard short characteristics approach (e.g. Kunasz and Olson, 1988), assuming Lagrangian parabolic approximation, the integral is expressed in terms of the source functions at three points: upwind ( $U$ ), local ( $L$ ) and downwind ( $D$ ) (the latter being the successive intersection point, see Fig. 1), so that Eq. (17) becomes:

$$I_L = I_U e^{-\Delta} + (\Psi_U S_U + \Psi_L S_L + \Psi_D S_D), \quad (18)$$

where the coefficients  $\Psi$  depend on the interpolation weights. Instead, short characteristics between two points  $U$  and  $L$  are employed in the FBILI. The integral is then expressed in terms of the source function at these two points and the source function derivative at local point  $L$ :

$$I_L = I_U e^{-\Delta} + p_L S_L + q_L S_U + r_L S'_L. \quad (19)$$

It is important to note that upwind point  $U$  is not the grid point and that the corresponding values of intensity and source function,  $I_U$  and  $S_U$ , must be evaluated by interpolation (see e.g. Auer and Paletou, 1994). The coefficients  $p_L$ ,  $q_L$  and  $r_L$  depend solely on  $\Delta$ , and thus implicitly on direction and frequency. If we assume a piecewise parabolic behavior of the source function, their values are given by:

$$p_L = 1 - \frac{2}{\Delta^2} + e^{-\Delta} \left( \frac{2}{\Delta} + \frac{2}{\Delta^2} \right) \\ q_L = \frac{2}{\Delta^2} - e^{-\Delta} \left( 1 + \frac{2}{\Delta} + \frac{2}{\Delta^2} \right) \\ r_L = -1 + \frac{2}{\Delta} - e^{-\Delta} \left( 1 + \frac{2}{\Delta} \right). \quad (20)$$

Let us note that the specific intensity  $I$  and the first derivative of the source function  $S'$  are the functions not only of the coordinates (like  $S$ ), but also of the direction and the frequency. The local derivative of the source function over the optical path length can be expressed in terms of partial derivatives with respect to  $x$  and  $y$ -axes, and in the case of unit opacity ( $\chi = 1$ ) can be cast into the form:

$$S'_L(v, \theta, \varphi) = \frac{1}{\phi(v)} \left[ \left( \frac{\partial S}{\partial x} \right)_L \cos \varphi \sin \theta + \left( \frac{\partial S}{\partial y} \right)_L \sin \varphi \sin \theta \right]. \quad (21)$$

The angles  $\theta$  and  $\varphi$  are shown in Fig.1.

Using Eq. (21), Eq. (19) can be written for each sweep as follows:

$$I_L = I_U e^{-\Delta} + p_L S_L + q_L S_U + r_{L,x} \left( \frac{\partial S}{\partial x} \right)_L + r_{L,y} \left( \frac{\partial S}{\partial y} \right)_L, \quad (22)$$

where the coefficients  $r_{L,x}$  and  $r_{L,y}$  follow directly from the above definition of the coefficient  $r_L$  and Eq. (21). Once the values of the specific intensity and the source function at the upwind point are obtained by interpolation and after computing the coefficients  $p_L, q_L, r_{L,x}$  and  $r_{L,y}$ , the only values that remain to be computed are the local partial derivatives of the source function with respect to  $x$  and  $y$ .

### 3.1.1. Computation of the derivatives

The partial derivatives at the local point are obtained by numerical differentiation. Here we use the Lagrangian interpolation of the second order at three successive points centered at the local one, that is:

$$\left( \frac{\partial S}{\partial x} \right)_{i,j} = w_{i-1,j,x} S_{i-1,j} + w_{i,j,x} S_{i,j} + w_{i+1,j,x} S_{i+1,j}, \quad (23)$$

and

$$\left( \frac{\partial S}{\partial y} \right)_{i,j} = w_{i,j-1,y} S_{i,j-1} + w_{i,j,y} S_{i,j} + w_{i,j+1,y} S_{i,j+1}. \quad (24)$$

The explicit expressions for the weights in Eq. (23) are:

$$\begin{aligned} w_{i-1,j,x} &= \frac{(x_i - x_{i+1})}{(x_{i-1} - x_i)(x_{i-1} - x_{i+1})} \\ w_{i,j,x} &= \frac{1}{x_i - x_{i+1}} + \frac{1}{x_i - x_{i-1}} \\ w_{i+1,j,x} &= \frac{(x_i - x_{i-1})}{(x_{i+1} - x_i)(x_{i+1} - x_{i-1})} \end{aligned} \quad (25)$$

The weights used in Eq. (24) have the same form, except they depend on the discrete values of  $y$ . At the boundaries of the grid, linear approximation is used. Let us note that the local source function  $S_{i,j}$  contributes to the local partial derivatives, so that the corresponding weights can be summed up with the coefficient  $p_L$  in Eq. (22). In some of the iterative procedures described in the next section this led to a better stability and improved the convergence rate of the method.

The formal solution given above will be implemented in the different iterative schemes described in the next section.

### 3.2. Iterative procedures

Let us recall again that the simplest iterative scheme,  $\Lambda$  iteration, computes the mean intensity ( $J = \Lambda S$ ) and the source function ( $S = S(J)$ ) in turn. In order to compute the mean intensity at any grid point it is necessary to

perform four sweeps of the grid, i.e. to compute the specific intensities (using Eq. (22)) at all the grid points along each sweep with the old values of the source function known from the previous iteration. Once the mean intensities at all grid points are obtained, one can compute new source function using Eq. (16). Iterations are repeated until the convergence is achieved. As already mentioned, this is an extremely slow procedure because it transfers from one part of the iterative step to the other more information than necessary. In what follows we will explain how  $\Lambda$  iteration in 2D has been accelerated up to now and how it can be further accelerated by our approach. More specifically, we will describe our implementation of Jacobi and Gauss–Seidel methods, and two variants of the FBILI procedure applied to 2D line transfer problem.

#### 3.2.1. Jacobi-type iteration

An efficient way to accelerate the  $\Lambda$  iteration is to simplify the treatment of the RT process, fully described by the exact Lambda operator, by replacing the latter with an approximate lambda operator  $\Lambda^*$  (ALO). The errors introduced by this approximation are then corrected iteratively. By using the “operator splitting” techniques (well-known from numerical analysis) we can rewrite the formal solution of the RT equation in the form:

$$J = \Lambda S = (\Lambda - \Lambda^*)S + \Lambda^* S. \quad (26)$$

Olson et al. (1986) were the first to point out that the diagonal of the exact  $\Lambda$  matrix itself represents an almost optimum ALO.

In the following we will describe a Jacobi-type iterative procedure and show that the coefficients  $b_L$  of the local source function play the role of the diagonal ALO in the Jacobi method.

In our Jacobi-type procedure applied to 2D radiative transfer, first we have to sweep the grid 4 times, and in every sweep  $k$  to compute and store the coefficients of the linear relation:

$$J_L^k = a_L^k + b_L^k S_L. \quad (27)$$

This equation is obtained by the angle- and line profile integration of Eq. (22), in such a way that the coefficients  $a_L^k$  contain all the non-local contributions to the specific intensity at the given point  $L$ :

$$a_L^k = \frac{1}{4\pi} \int_{-\infty}^{\infty} \phi(v) dv \int \left[ I_U^k e^{-\Delta^k} + q_L^k S_U^k + r_{L,x}^k \left( \frac{\partial S}{\partial x} \right)_L^k + r_{L,y}^k \left( \frac{\partial S}{\partial y} \right)_L^k \right] d\Omega, \quad (28)$$

and are computed using the current values of the source function and its derivatives, whereas the coefficients  $b_L^k$ , which play the role of the diagonal ALO, have the form:

$$b_L^k = \frac{1}{4\pi} \int_{-\infty}^{\infty} \phi(v) dv \int p_L^k d\Omega, \quad (29)$$

To be consistent, the contribution of the local source function to the local partial derivatives (see Eqs. (23) and (24)) should be included in the coefficient  $b_L^k$  rather than in the coefficient  $a_L^k$ .

The total mean intensity at point  $L$  is obtained by summing up the mean intensities in all the sweeps, and is given by

$$J_L = a_L + b_L S_L, \quad (30)$$

where  $a_L = \sum_{k=1}^4 a_L^k$  and  $b_L = \sum_{k=1}^4 b_L^k$  are the total coefficients.

Once we know the coefficients of Eq. (30), by inserting Eq. (30) into Eq. (16) we can update the source function at all depth points throughout the 2D grid by means of:

$$S_L = \frac{\varepsilon B + (1 - \varepsilon) a_L}{1 - (1 - \varepsilon) b_L}. \quad (31)$$

In this way, the iterative computation of the coefficients  $a_L$  and  $b_L$  of the implicit relation (30) instead of the unknown quantities ( $J_L$  and  $S_L$ ) themselves leads to much more efficient corrections than in  $\Lambda$  iteration. This scheme reduces the number of iterations by a few orders of magnitude with respect to the ordinary  $\Lambda$  iteration. However, even this is not fast enough for some more demanding problems (strong, scattering dominated lines).

### 3.2.2. Gauss–Seidel-type iteration

As it has just been explained, in the Jacobi iteration the grid is swept four times and in every sweep the coefficients  $a_L^k$  and  $b_L^k$  are computed from the “old” values of the source function. Only after getting the total coefficients  $a_L$  and  $b_L$  at all grid points, the source function is updated using Eq. (31).

The Jacobi scheme can be substantially accelerated if the new source function is computed as soon as the total coefficients  $a_L$  and  $b_L$  in Eq. (30) are available (known) at some point. This is, for example, the situation at the boundary grid points after sweeping the grid three times and computing the corresponding coefficients  $a_L^k$  and  $b_L^k$  ( $k = 1, 3$ ). We start the fourth sweep with given values of  $a_L^4$  and  $b_L^4$  at two boundaries:  $(1, j)$ ;  $j = 1, NY$  and  $(i, NY)$ ;  $i = 1, NX$  (see Fig. 3). The new source function  $S_L$  at these points is easily computed using Eq. (31). As the sweep goes on, the values of the source function at subsequent points are progressively computed. The use of these updated values in the computation of the local intensities along the fourth sweep accelerates the convergence of the method. This numerical scheme corresponds to the Gauss–Seidel method known from numerical algebra (see e.g. Saad, 2003). For the solution of the 1D NLTE RT problem this idea was implemented in two different ways by Trujillo Bueno and Fabiani Bendicho (1995) and ACS97. In the paper by Trujillo Bueno and Fabiani Bendicho (1995) a standard approximate  $\Lambda$  operator approach with three-point algorithm to set up short characteristics of the second order is used. This method has been explicitly generalized to 2D geometry by Léger et al. (2007). The FBILI method,

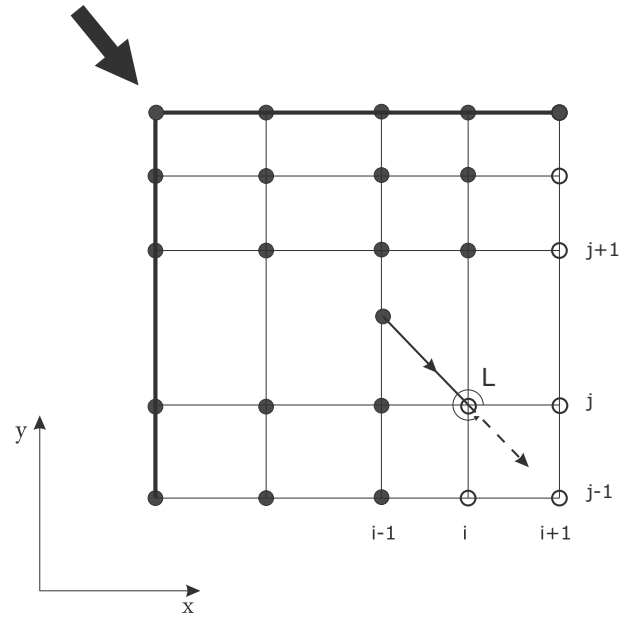


Fig. 3. 2D grid sweep in the 4th direction. Full dots correspond to the new values of the source function, empty ones to the old values. The boundary conditions are defined at  $L(1, j)$ ,  $j = 1, NY$  and at  $L(i, NY)$ ,  $i = 1, NX$ .

developed by ACS97, uses a two-point algorithm and computes the coefficients of the implicit relations expressing the intensities in terms of the source functions and its derivatives at pairs of successive depth points.

The whole procedure is more complicated in multidimensional geometries because of the spatial interpolations needed to obtain values of the upwind source function and intensities. Let us consider the 2D procedure in more detail.

Fig. 3 illustrates the situation when the fourth (last) sweep arrives at the grid point  $(i, j)$ , after the 2D grid has been swept three times. We assume that the source function has been already updated at the points represented by full dots. From now on we will refer to the sweeps during which the formal solution is performed, and appropriate coefficients are stored, with no correction of the source function as the *forward* sweeps, whereas the sweeps during which the source function is updated as the *backward* ones.<sup>2</sup>

It is essential to realize that all the non-local contributions to the coefficient  $a_L$  in Eq. (31) must be properly taken into account. Some of these contributions have been already updated in the current sweep (“new”), while the others still have their values from the previous iteration (“old”).

In our implementation of Gauss–Seidel iterative scheme we first modify the formal solution in the following way: We use Eq. 22 with partial derivatives given by Eqs. (23) and (24), thus expressing explicitly the contributions of

<sup>2</sup> For example, Jacobi iteration consists of four forward sweeps followed by the simultaneous update of the source function over the entire grid.

$S_{i-1,j}, S_{i+1,j}, S_{i,j-1}$  and  $S_{i,j+1}$  to the local specific intensity. Furthermore, upwind source function  $S_U$  is also expressed in terms of the source function values at the neighboring grid points. As an example, for the point  $U_1$  in Fig. 2 we have:

$$S_U = W_{i-1,j-1}S_{i-1,j-1} + W_{i,j-1}S_{i,j-1} + W_{i+1,j-1}S_{i+1,j-1}. \quad (32)$$

In the above equation the weights  $W$  follow from the Lagrangian interpolation of the second order, and, for convenience, we give the expressions:

$$\begin{aligned} W_{i-1,j-1} &= \frac{(x_U - x_i)(x_U - x_{i+1})}{(x_{i-1} - x_i)(x_{i-1} - x_{i+1})}, \\ W_{i,j-1} &= \frac{(x_U - x_{i-1})(x_U - x_{i+1})}{(x_i - x_{i-1})(x_i - x_{i+1})}, \\ W_{i+1,j-1} &= \frac{(x_U - x_{i-1})(x_U - x_i)}{(x_{i+1} - x_{i-1})(x_{i+1} - x_i)}. \end{aligned} \quad (33)$$

Finally, Eq. (22) for each sweep  $k$  takes the new form:

$$I_L^k = I_U^k e^{-\Delta^k} + p_L^k S_L + \sum_{i'} \sum_{j'} r_{i',j'}^k S_{i',j'}. \quad (34)$$

The expression for the parabolic interpolation formula in the above equation is similar to the one given by Eq. (5) in the paper by Kunasz and Auer (1988). Here the coefficients  $r_{i',j'}$  depend on the approximations used to compute the local derivative of the source function  $S'_L$  and to interpolate the value of the source function at upwind point  $S_U$ . Note that  $r_{i,j}$  (indices  $(i,j)$  refer to the grid point  $L$ ) is always zero, as all local contributions are added to the coefficient  $p_L$ . In this way, all the non-local contributions (in all sweeps) except the upwind specific intensities are explicitly expressed using eight neighboring source functions.

Integration of Eq. (34) over angles and line profile yields:

$$J_L^k = a_L^k + b_L^k S_L + \sum_{i'} \sum_{j'} c_{i',j'}^k S_{i',j'}. \quad (35)$$

Here, the coefficients are defined as:

$$a_L^k = \int \phi(v) dv \int \frac{d\Omega}{4\pi} I_U^k e^{-\Delta^k}, \quad (36)$$

$$b_L^k = \int \phi(v) dv \int \frac{d\Omega}{4\pi} p_L^k, \quad (37)$$

and

$$c_{i',j'}^k = \int \phi(v) dv \int \frac{d\Omega}{4\pi} r_{i',j'}^k. \quad (38)$$

After computing the coefficients  $a_L^k, b_L^k$  and  $c_{i',j'}^k$  in all four directions, the source function can be updated according to:

$$S_L = \frac{\varepsilon B + (1 - \varepsilon) \left( a_L + \sum_{i'} \sum_{j'} c_{i',j'} S_{i',j'} \right)}{1 - (1 - \varepsilon) b_L}, \quad (39)$$

where  $a_L = \sum_k a_L^k, b_L = \sum_k b_L^k$  and  $c_{i',j'} = \sum_k c_{i',j'}^k$ .

Let us point out here that the upwind intensity  $I_U^4$ , contained in the coefficient  $a_L^4$ , is computed from the updated source function at previous points along the fourth sweep. It is important to stress that if Eq. (39) is used to update the source function in the backward sweep, all the proper contributions of “new” and “old” neighboring source functions are *automatically* taken into account, through the sum  $\sum_{i'} \sum_{j'} c_{i',j'} S_{i',j'}$ . We now propose the following, Gauss–Seidel like scheme:

1. Sweep the grid in the first three directions (forward sweeps), computing and storing the corresponding coefficients  $a_L^k, b_L^k$  and  $c_{i',j'}^k$ , ( $k = 1, 3$ ) of Eq. (35) by means of the old values of the source function.
2. Start the fourth (backward) sweep. At the grid points on the two boundaries (i.e. the points  $L = (1, j)$  and  $L = (i, NY)$ , marked in bold in Fig. 3), specific intensities of the incident radiation field are known so that  $a_L^4, b_L^4$  and  $c_{i',j'}^4$  are known, and the source function  $S_L$  can be straightforwardly computed using Eq. (39). After updating the source function, specific intensity  $I_L^4$  is computed using Eq. (34).
3. At all the subsequent points of the backward sweep, with the updated values of the specific intensities  $I_L^4$  at previous points, the upwind intensity  $I_U^4$  is to be computed, and, hence the coefficient  $a_L^4$ . Once the total coefficients  $a_L, b_L$  and  $c_{i',j',L}$  are obtained, the source function is updated by means of Eq. (39) and specific intensity is computed using Eq. (34).
4. Steps 1–3 are repeated until convergence.

The main difference between this scheme and the above described Jacobi-like scheme is that the source function is updated *in the course* of the fourth sweep (instead *after* the fourth sweep is completed). This modification introduced by the Gauss–Seidel approach significantly increases the rate of convergence. As we shall see in the next section, even further acceleration in 2D is possible by the application of the forth-and-back approach and the use of iteration factors.

### 3.2.3. “Two-by-two” FBILI method

FBILI method proposed by ACS97 brought about improvements upon the existing techniques because of: (i) the iterative computation of the coefficients of the implicit linear relation between the specific intensities and the local source function and its derivative in the forward sweep, combined with an efficient method of back-substitution (a two-point, not a three-point scheme), which led to a quick update of  $S$  and  $S'$  along the 1D grid, and (ii) the use of the iteration factor  $((I_U e^{-\Delta} + q S_U) / S_L)$  in the forward sweep, which “enhances” the local operator. This resulted in an extremely fast convergence with respect to the previous schemes. The acceleration of the iterative procedure is due to the fact that it is much faster to iterate on the ratio



of the unknowns than on the unknowns themselves.<sup>3</sup> In 1D case, introduction of the iteration factor increased the convergence rate of the FBILI method by a factor of 4.

In order to generalize FBILI to 2D we ought to take into account that, due to the twofold two-point boundary nature of the problem, we have two pairs of the mutually opposite sweeping directions (1–3 and 2–4). We can, therefore, emulate the original FBILI approach by considering two inward directions (1 and 2) as the forward ones and two outward directions (3 and 4) as the backward ones. The update of the source function is thus performed twice during the single iteration. Moreover, in the forward sweeps we can introduce appropriate iteration factors into the ‘local’ coefficient  $b_L$  to speed up the convergence.

In general, the method can be used in many different ways: it is possible to use iteration factors in one or two sweeps, or not at all; there can be one, two, or even four backward sweeps. In the following we present some of the most efficient schemes.

As before, we use Eqs. (34) and (35), and we include the iteration factors in the computation of the coefficient  $b_L$  during the two in-going (forward) sweeps 1 and 2:

$$b_L^{1,2} = \int \phi(v) dv \int \left( p_L^{1,2} + \frac{I_U^{1,2} e^{-\Delta^{1,2}}}{S_L^{\text{old}}} \right) d\Omega, \quad (40)$$

while in the out-going (backward) sweeps the coefficient  $b_L$  contains only angle- and line profile-integrated coefficient  $p_L$  from Eq. (34).

We propose the following iteration procedure:

1. Sweep the grid three times (forward sweeps), computing the specific intensity by means of Eq. (34) and iteration factors in directions 1 and 2 as given by Eq. 40. Compute the corresponding coefficients  $a_L^{1-3}$ ,  $b_L^{1-3}$  and  $c_{ij}^{1-3}$ .
2. In the fourth (backward) sweep, starting from the grid points on two corresponding boundaries with known boundary conditions, update the source function by means of Eq. (39) and the out-going specific intensity using Eq. (34) point by point throughout the grid.
3. Sweep the grid in direction 1 (iteration factor is used).
4. Sweep the grid in direction 3 (no iteration factor).  
*Update the source function and the intensity while performing the sweep.* Note that this sweep is now backward sweep.
5. Sweep the grid in direction 2 (iteration factor is used).
6. Sweep the grid in direction 4 (no iteration factor).  
*Update the source function and the intensity while performing the sweep.*
7. Repeat steps 3–6 until convergence.

The only differences in the above scheme, with respect to our GS-like procedure described in Section 3.2.2 are: (a)

inclusion of the iteration factors in the (in-going) sweeps 1 and 2; (b) a reordering of the sweeps (1–3–2–4) and (c) updating of the source function in the (out-going) sweeps 3 and 4, i.e. there are two backward sweeps now instead of just one. Hence, the source function is updated twice per iteration, i.e. once per each pair of the mutually opposite sweeping directions (1–3 and 2–4). This implementation shows a very good stability and also much better convergence properties with respect to other methods described previously. This inspired us to try to further accelerate the method by updating the source function *in all four sweeps*.

### 3.2.4. “Sweep by sweep” FBILI procedure

In the previous section we have seen that the update of the source function can be performed more than once during a single iteration. This idea was realized in 1D plane-parallel geometry by means of SSOR (symmetric successive overrelaxation) method (see, for example: Samproorna and Trujillo Bueno, 2010). In principle, as soon as the grid is swept four times in the first iteration and coefficients  $a^{1-4}$ ,  $b^{1-4}$  and  $c_{ij}^{1-4}$  are known, one can update the source function in *every* sweep of the grid.

Here, the only difference with respect to the “two-by-two” procedure is that after the step 2, the source function is updated during all four sweeps (“sweep by sweep”). This leads to four updates per iteration at essentially no additional computational cost (computation of the source function takes a negligible time with respect to the formal solution). This very same procedure without iteration factors would correspond to the Symmetric Gauss–Seidel (SGS) method in 2D geometry. As we will see in the next section, this method, with the help of iteration factors, extremely accelerates the convergence with no additional numerical acceleration technique.

## 4. Results

In order to test the properties of the above mentioned procedures we solved the problem given by Auer and Paletou (1994). We considered a slab of the optical depth  $\tau = 10^4$  along both ( $x$  and  $y$ ) axes, with  $\varepsilon = 10^{-4}$  and  $B = 1$ . Equidistant logarithmic spacing in optical depth with approximately 10 points per decade ( $129 \times 129$  points) is used. The slab is irradiated at the bottom and on both sides, from the angles  $\pi < \varphi < 2\pi$ , with the radiation equal to  $B$ . For the discretization in angle we used Carlson’s set B (Carlson, 1963) with  $n = 8$  (12 angles per octant). For the frequency quadrature the trapezoidal rule is used with nine frequency points in a half of the Doppler line profile.

The convergence properties of the iterative procedures are analyzed by calculating at each iteration step  $i$  the maximum relative change of the source function between two successive iterations  $i - 1$  and  $i$ :

$$R_c^i = \left| \frac{S^i - S^{i-1}}{S^i} \right|_{\max}. \quad (41)$$

<sup>3</sup> This refers to the iteration factor, but also, in a way, to the coefficients of the implicit relations.

The first tested procedure, denoted here as the Jacobi-type procedure, needed 118 and 195 iterations to reach the maximum relative changes  $R_c = 10^{-3}$  and  $R_c = 10^{-5}$ , respectively. It is evident that higher convergence rate is desired. As mentioned before, it is customary to apply the Ng acceleration (Ng, 1974) to the Jacobi method. However, since its implementation is not straightforward (it requires some preliminary numerical tests and analysis) we have not used it, i.e. we present here the results with no additional mathematical acceleration techniques like the Ng's.

When we applied the Gauss–Seidel type procedure we obtained the corresponding solutions in 77 and 126 iterations. The increase in the convergence rate is evident, but not as great as in 1D case.

Finally, two FBILI procedures that use iteration factors (“2-by-2” and “sweep-by-sweep”) dramatically increased the convergence rate (see Fig. 4). In these procedures, we define one iteration as the whole set of four sweeps, although the source function is updated two (four) times (recall that the computation of the source function is very fast). The “two-by-two” FBILI that employs the iteration factors in two ‘inward’ sweeps and updates the source function in two ‘outward’ sweeps, achieves the maximum relative change  $R_c = 10^{-3}$  in 28 iterations and  $R_c = 10^{-5}$  in 44 iterations. We see that the convergence rate of this scheme is higher than that of the Jacobi method by a factor of four. The “sweep-by-sweep” procedure that employs the iteration factors in two ‘inward’ sweeps updating the source function in all four sweeps achieves the above maximum relative changes in 19 and 29 iterations, respectively (i.e. 6–7 times faster than the Jacobi scheme). The “sweep-by-sweep” scheme without iteration factors, i.e. the generalization of the SGS-type method, satisfies the above convergence criteria in 39 and 61 iterations, respectively. The importance of the iteration factors is evident, as they improve the convergence rate of the SGS method by a factor of more than two.

In order to study the performance of an iterative method, also the maximum relative true error ought to be

analyzed. Since the analytical solution of this benchmark problem cannot be obtained, the true accuracy of a method is expressed with respect to  $S_{\text{REF}}^{\infty}$  – the fully converged ‘exact’ solution obtained with some well-tested reference (REF) code in the finest spatial grid:

$$T_e^i = \left| \frac{S^i - S_{\text{REF}}^{\infty}}{S_{\text{REF}}^{\infty}} \right|_{\text{max}}. \quad (42)$$

In this case we used as the “exact” solution the result obtained in the 2000th Jacobi iteration ( $R_c \approx 10^{-13}$ ), with an extremely fine grid (i.e. a grid with 40 points per decade). Considering that the source function along the central line of the slab,  $S(NX/2, j)$ ;  $j = 1, NY$ , has a similar behavior to the solution in a 1D semi-infinite stellar atmosphere, we took the central surface point  $(NX/2, 1)$  as the point of interest in analyzing the true error.

The variation of the maximum relative true error  $T_e$  with the iteration number is shown in Fig. 5 for all the procedures considered. After a rapid initial improvement  $T_e$  exhibits an asymptotic behavior with iterations, reaching the so-called truncation error  $T_e(\infty)$  (a measure of the true accuracy) of about 0.35%. From Figs. 4 and 5 we see that the iterations can be stopped once the criterion  $R_c < 0.1T_e(\infty)$  is satisfied (see Auer et al., 1994), as the further decrease in relative corrections does not increase the accuracy achieved any more. Note here that Auer and Paletou (1994) used  $\Delta S/S < 10^{-2}\epsilon$  as their stopping criterion.

From Fig. 5, excellent properties of the FBILI method are again evident. For a fast convergent method such as this one, one can actually use a weaker convergence criterion in terms of  $R_c$ . To make this statement clear, recall that a slowly converging method may reach small relative change quickly being, however, far from the “true” solution. In principle, the true error should be used for setting the convergence criterion, but as it is not known, good knowledge of the convergence properties of the method in question must be obtained in order to set the proper value of  $R_c$  as the convergence criterion, thus optimizing the computing time.

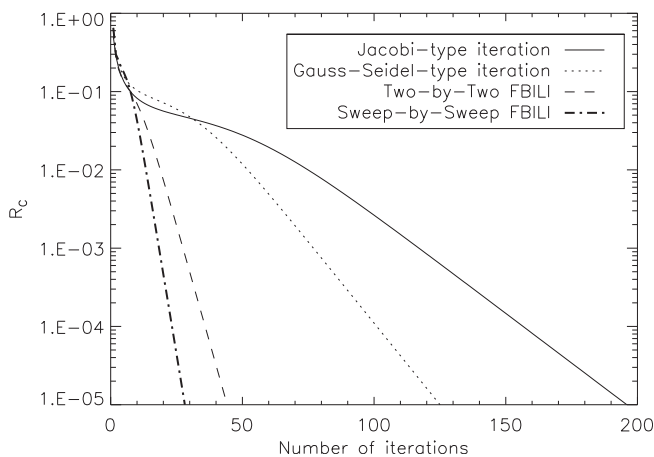


Fig. 4. Variation of the maximum relative change with iterations for the iterative procedures considered.

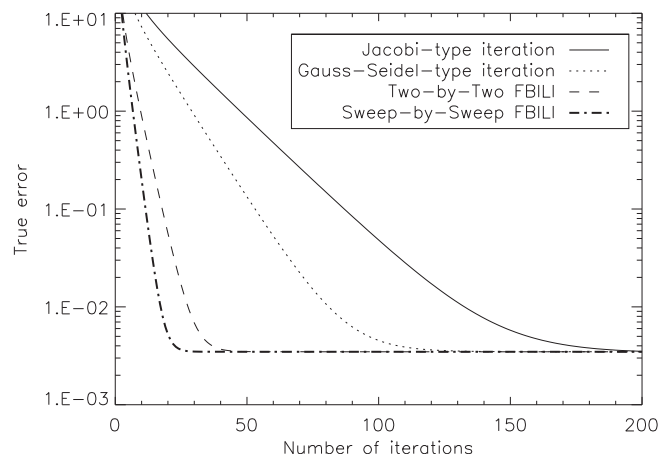


Fig. 5. Variation of the true error with iterations for the procedures considered.

## 5. Conclusions

We have presented a new iterative scheme for the NLTE line radiative transfer in 2D Cartesian geometry. It uses the basic ideas of the FBILI method developed previously for 1D radiative transfer problems. The proposed iterative procedure dramatically increases the convergence rate with respect to the existing techniques by introduction of the iteration factor in the ‘local’ coefficient of the linear relation between the mean intensity  $J$  and the corresponding source function  $S$  (in two ‘inward’ sweeps of the grid), along with the use of new values of the source function as soon as they are available (in all four sweeps).

Even better comparative convergence properties of the FBILI method can be expected in applications to some more realistic problems; e.g. in the semi-infinite atmosphere with periodic boundary conditions. Just as 1D FBILI iterative scheme shows its full advantage for optically thick media and scattering dominated problems that need fast methods to be solved efficiently, we are aimed at achieving the same with FBILI generalized to the 2D and 3D cases. Our first goal is to implement the periodic boundary conditions in the code and also to test more accurate interpolating strategies (for example, cubic interpolation, as suggested by [Simonneau et al. \(2012\)](#)) in computing the formal solution, the source function derivatives, and the spatial interpolation at the upwind point. We are aimed at generalizing the backward elimination scheme from 1D FBILI to 2D more straightforwardly, expressing the local derivative in terms of the updated values of the source function and its derivative at previous grid points. This would eliminate the need for keeping eight  $c_{if}$  coefficients and lead to more elegant solution.

In the future work we will also test the scaling of the convergence properties with respect to grid resolution and demonstrate the generalization of the method to the multilevel atom case, and to polarized line transfer with PRD in a two-level atom approximation as well.

## Acknowledgements

We thank Marianne Faurobert for useful discussions during IM’s and OA’s stay in Nice. We are indebted to anonymous referees, not only for useful comments on an earlier version of this manuscript, but also for pointing us possible improvements of our method. This research is being done in the framework of the Project 176004, “Stellar Physics”, supported by the Serbian Ministry of Science and Education.

## References

- Anusha, L.S., Nagendra, K.N., 2011. Polarized line formation in multi-dimensional media. I. Decomposition of Stokes parameters in arbitrary geometries. *ApJ* 726, 6–18.
- Anusha, L.S., Nagendra, K.N., Paletou, F., 2011. Polarized line formation in multi-dimensional media. II. A fast method to solve problems with partial frequency redistribution. *ApJ* 726, 96–108.

- Atanacković-Vukmanović, O., 2007. Solution of NLTE radiative transfer problems using forth-and-back implicit lambda iteration. In: Demircan, O., Selam, S.O., Albayrak, B. (Eds.), *Solar and Stellar Physics Through Eclipses*, ASP Conference Series, vol. 370, pp. 97–102.
- Atanacković-Vukmanović, O., Crivellari, L., Simonneau, E., 1997. A forth-and-back implicit  $\Lambda$ -iteration. *ApJ* 487, 735–746.
- Auer, L.H., Paletou, F., 1994. Two-dimensional radiative transfer with partial frequency redistribution I. General method. *A&A* 285, 675–686.
- Auer, L.H., Fabiani Bendicho, P., Trujillo Bueno, J., 1994. Multidimensional radiative transfer with multilevel atoms. I: ALI method with preconditioning of the rate equations. *A&A* 292, 599–615.
- Carlson, B.G., 1963. In: Adler, B., Fernbach, S., Rotenberg, M. (Eds.), *Methods in Computational Physics*, Vol. 1. Academic Press, New York.
- Faurobert-Scholl, M., Frisch, H., Nagendra, K.N., 1997. An operator perturbation method for polarized line transfer. I. Non-magnetic regime in 1D media. *A&A* 322, 896–910.
- Hayek, W., Asplund, M., Carlsson, M., Trampedach, R., Collet, R., Gudiksen, B.V., Hansteen, V.H., Leenaarts, J., 2010. Radiative transfer with scattering for domain-decomposed 3D MHD simulations of cool stellar atmospheres. Numerical methods and application to the quiet, non-magnetic, surface of a solar-type star. *A&A* 517, A49.
- Hubeny, I., 2003. Accelerated lambda iteration: an overview. In: Hubeny, I., Mihalas, D., Werner, K. (Eds.), *Stellar Atmosphere Modeling*, ASP Conference Series, vol. 288, pp. 17–30.
- Kunasz, P.B., Auer, L.H., 1988. Short characteristic integration of radiative transfer problems – formal solution in two-dimensional slabs. *JQSRT* 39, 67–79.
- Kunasz, P.B., Olson, G.L., 1988. Short characteristic solution of the non-LTE line transfer problem by operator perturbation. II – The two-dimensional planar slab. *JQSRT* 39, 1–12.
- Léger, L., Chevallier, L., Paletou, F., 2007. Fast 2D non-LTE radiative modelling of prominences. Numerical methods and benchmark results. *A&A* 470, 1–9.
- Mihalas, D., 1978. *Stellar Atmospheres*, 2nd edition. W.H. Freeman and Co., San Francisco.
- Mihalas, D., Auer, L.H., Mihalas, B.R., 1978. Two-dimensional radiative transfer. I – Planar geometry. *ApJ* 220, 1001–1023.
- Milić, I., 2013. Transfer of polarized line radiation in 2D cylindrical geometry. *A&A* 555, A130.
- Ng, K.C., 1974. Hypernetted chain solutions for the classical one-component plasma up to Gamma equals 7000. *J. Chem. Phys.* 61, 2680–2689.
- Olson, G.L., Auer, L.H., Buchler, J.R., 1986. A rapidly convergent iterative solution of the non-LTE line radiation transfer problem. *JQSRT* 35, 431–442.
- Papkalla, R., 1995. Line formation in accretion disks 3D comoving frame calculations. *A&A* 295, 551–564.
- Saad, Y., 2003. *Iterative Methods for Sparse Linear Systems*, second ed. Society for Industrial and Applied Mathematics, Philadelphia, PA, USA.
- Samprorna M., Trujillo Bueno, J., R., 2010. Gauss-Seidel and Successive Overrelaxation Methods for Radiative Transfer with Partial Frequency Redistribution, *ApJ* 712, 1331–1344.
- Simonneau, E., Cardona, O., Crivellari, L., 2012. An improved version of the implicit integral method to solving radiative transfer problems. *Ap* 55, 110–126.
- Trujillo Bueno, J., Fabiani Bendicho, P., 1995. A novel iterative scheme for the very fast and accurate solution of non-LTE radiative transfer problems. *ApJ* 455, 646–657.
- van Noort, M., Hubeny, I., Lanz, T., 2002. Multidimensional non-LTE radiative transfer. I. A universal two-dimensional short-characteristics scheme for Cartesian, spherical, and cylindrical coordinate systems. *ApJ* 568, 1066–1094.